

## Overview of the Swiss Seismological Service's Efforts to Monitor the July 2025 Test-Stimulation in Haute-Sorne, Switzerland

Vanille A. Ritz<sup>1</sup>, Verónica Antunes<sup>1</sup>, Paolo Bergamo<sup>1</sup>, Toni Kraft<sup>1</sup>, Michèle Marti<sup>1</sup>,  
Philippe Roth<sup>1</sup>, Verena Simon<sup>1</sup>, Tania Toledo<sup>1</sup>, and Stefan Wiemer<sup>1</sup>

<sup>1</sup>Swiss Seismological Service at ETH Zurich, Zurich, Switzerland

[vanille.ritz@sed.ethz.ch](mailto:vanille.ritz@sed.ethz.ch)

**Keywords:** Enhanced Geothermal Systems, Seismic Risk, Seismic Monitoring, Induced Seismicity

### ABSTRACT

In Switzerland, the subsurface is under the sovereignty of the 26 different cantons, with cantonal authorities in charge of the permitting and regulatory oversight of industrial projects targeting the subsurface. The GEOBEST program ensures that the Swiss Seismological Service at ETH Zurich can provide seismological expertise and baseline seismic monitoring services to the cantons at no cost, and independently of the operators of geothermal projects.

For the EGS pilot project in Haute-Sorne, the Republic and Canton of Jura receives the support of the Swiss Seismological Service with seismological consulting and risk governance recommendations, as well as the operation of a dedicated seismic network. This seismic network completed in February 2024 consists of seven stations (broadband and strong motion) and was designed to ensure a magnitude of completeness of at least  $M_{Lhc}0.5$ . The test-stimulation carried out in July 2025 saw 430 m<sup>3</sup> of water injected at nearly 4 km depth with injection rates up to 80L/min. During this period, the Swiss Seismological Service provided 24/7 automatic alarms in a 4 km radius with manual revision within the hour. These alarms fed the magnitude-based traffic light system operated by Geo-Energie Jura, the operator of the Haute-Sorne project.

### 1. INTRODUCTION

Switzerland's Energy Strategy 2050 outlines a comprehensive transition of the national energy system to support long-term decarbonization and achieve the stated net-zero greenhouse gas emissions target by 2050. The strategy approved by referendum in 2017 aims to restructure the energy system by increasing energy efficiency, expanding domestic renewable energy production, phasing out nuclear power, and reducing dependence on fossil imports. In this framework, deep geothermal energy is projected to contribute to the energy mix (both for electricity and heat), with an objective to provide 4.4TWh annually by 2050. Geothermal energy offers a low-carbon baseload resource, ideal to complement hydropower and variable renewables in the decarbonized Swiss grid (Merkofer et al., 2024).

The exploitation of deep geothermal energy can, however, be constrained by induced seismicity, in particular in the case of Enhanced Geothermal Systems in which the reservoir is stimulated by injection operations in order to create or improve pathways for fluid to travel through the rock mass and heat up (Ellsworth, 2013). If low-magnitude induced events can serve as indicators of the reservoir development, unwanted large events can halt projects as seen in the examples of Basel (2006, Switzerland; Häring et al., 2008) or Pohang (2017, Republic of Korea; Grigoli et al., 2018). Measures of risk reduction include targeted hazard and risk modeling (e.g. van Elk et al., 2019) in the planning and operation phases as well as the rigorous monitoring of the seismicity, with alarming and mitigation actions to be put in place to avoid undesired events. One such mitigation can take the shape of traffic light systems (TLS) which aim at limiting the probability of felt or damaging seismic events by reducing and/or stopping operations early on before seismicity reaches intolerable levels, thus protecting public safety and infrastructure, and maintaining regulatory and societal acceptance (Bommer et al., 2006).

In Switzerland, the subsurface is under the sovereignty of the 26 different cantons, with cantonal authorities in charge of the permitting and regulatory oversight of industrial projects targeting the subsurface. In the framework of the GEOBEST2020+ project, funded by the Swiss Federal Office of Energy (SFOE), the Swiss Seismological Service (SED) at ETH Zurich supports the Republic and Canton of Jura in handling induced seismicity for deep geothermal projects in the canton. Part of this support is to provide the cantonal authorities and, indirectly, the operators with independent seismic baseline monitoring, and earthquake alarms for the deep geothermal projects in the canton (Kraft et al., 2025; Lupi et al., 2025). In the wider perspective of SED initiatives assisting decision-making in geothermal projects, it is also worth mentioning the extension of the national earthquake risk model (ERM-CH23, Papadopoulos et al., 2024) to shallow induced seismicity in the form of an Induced Earthquake Risk Model of Switzerland (IERM-CH25, Grigoratos et al., 2025; Bergamo et al., 2025).

### 2. THE HAUTE-SORNE EGS PROJECT

The Haute-Sorne Enhanced Geothermal System (EGS) pilot project, operated by Geo-Energie Jura and Geo-Energie Suisse, is a deep geothermal development located in the Jura region of Switzerland. The project aims to construct a geothermal power plant with a maximum electrical capacity of 5 MW. The reservoir is planned to be stimulated with a multi-stage concept, developed to reduce the risk of large induced seismicity by limiting the areas of hydraulically stimulated fracture planes (Meier et al., 2015; 2025). At full capacity, the plant is expected to produce approximately 40 GWh of electricity per year, corresponding to the annual consumption of more than 6,000 households.

Project development for the Haute-Sorne EGS pilot began in 2012 with site selection, followed by extensive planning, comprehensive geological and environmental studies, and stakeholder engagement between 2013 and 2015. Drilling operations of the first well of the doublet started in May 2024 and reached the target depth of 4 km in August 2024.

## 2.1 Project classification and risk governance framework

The good-practices guide of the SED recommends the use of an initial screening tool to classify geothermal projects based on the extent of concern that induced seismicity represents. This GRID tool (Geothermal Risk of Induced seismicity Diagnosis, Trutnevyte & Wiemer, 2017) evaluates projects based on three main dimensions: seismic hazard, seismic risk (including secondary hazards, exposure, and vulnerability), and social concern. The analysis is conducted by the three main seismicity-stakeholders of a project: the operator, the cantonal authorities, and the SED. Geothermal projects are classified in four categories, with category 0 representing the lowest level of concern, and category III, the highest. Figure 1 presents the GRID scores for the Haute-Sorne EGS project.

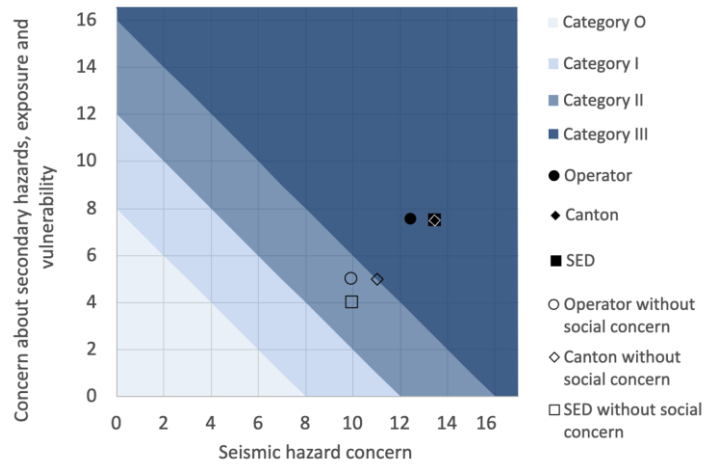


**Figure 1: GRID scores for the Haute-Sorne EGS place the project in category III. Circles: Operator (GES), diamond: Cantonal authorities, square: Swiss Seismological Service (SED). Filled symbols account for the third dimension of the GRID analysis (“Social concern”).**

Depending on the classification of the project, a framework of risk governance measures including seismic hazard and risk assessment, seismic monitoring requirements, mitigation measures, insurance and retrofitting criteria as well as public and stakeholder communication and engagement is recommended. The recommendations for each category are summarized in the good-practice guide by Kraft et al. (2025). On account of opposition to the project from a small but vocal group of local residents (Meier et al., 2025), the Haute Sorne EGS project was classified by all parties in category III. This classification implied strict requirements for the assessment of the seismic risk and hazard, insurance coverage, as well as completeness of the seismic monitoring.

## 2.2 Test stimulation

After the successful drilling of a first vertical well down to 4 km in Spring-Summer 2024, a first test stimulation was performed between July 8<sup>th</sup> and 15<sup>th</sup> 2025 to assess the response of the reservoir. This stimulation was performed in a perforated interval between depths 3800 and 3825 m, with 430 m<sup>3</sup> of water injected at rates not exceeding 80L/min and pressures up to 27 MPa. The injection test was followed by a period of flowback to reduce pressure in the reservoir and thus lower the seismic risk (Meier et al., 2025; Bethmann et al., 2025).

During this test stimulation, the SED operated its own seismic network and provided automated alarms for events to the operator and canton. A traffic light system was operated by GES/GEJ from these alarms and additional criteria. The following section covers the design and deployment of the SED’s seismic network as wells as the alarming system in place.

## 3. SEISMIC MONITORING AND ALARMING

### 3.1 Seismic network design

Since 2022, the SED has been cooperating with the canton Jura to install a seismological network which represents the backbone of the baseline monitoring network designed to insure a magnitude of completeness of at least  $M_{Lhc}0.5$  (in accordance to the GRID category III) and a location precision of 500 m horizontally and 2 km vertically in the Haute-Sorne alarming perimeter.

The design of the baseline monitoring network operated by the SED was decided based on simple network geometry principles: A central station at a distance of less than 2 km and four peripheral stations at ~10 km distance from the geothermal well in a quadripartite geometry following a set workflow (Antunes et al., 2025). In order to ensure the target magnitude of completeness prior to operations, we estimated the completeness using the Bayesian Magnitude of Completeness calibrated for Switzerland (BMC; Mignan et al., 2011; Kraft et al., 2013). Figure 2 shows the monitoring network and the estimated BMC in the 4 km alarming perimeter. The location accuracy is also verified by generating and locating a synthetic catalogue of events using a linearized earthquake location method, considering body wave travel times estimates and their derivatives and the long-term noise levels of all available stations. Figure 3 shows the predicted location precision for an event of  $M_{Lhc}0.0$  located at 5 km depth using a stress drop of 0.3 MPa (Bay et al., 2005).

3.2 Surface seismic network

The network completed in February 2024 consists of seven broadband seismic stations (three existing and four newly deployed), with seven additional stations deployed by the project operator and integrated in the SED network for improved quality in the direct vicinity of the project. Figure 2-a presents the network, with the colors indicating the SED stations (CH-red and G2-blue; Swiss Seismological Service 1983; 2006), and operator stations (5A-orange; Swiss Seismological Service, 2021).

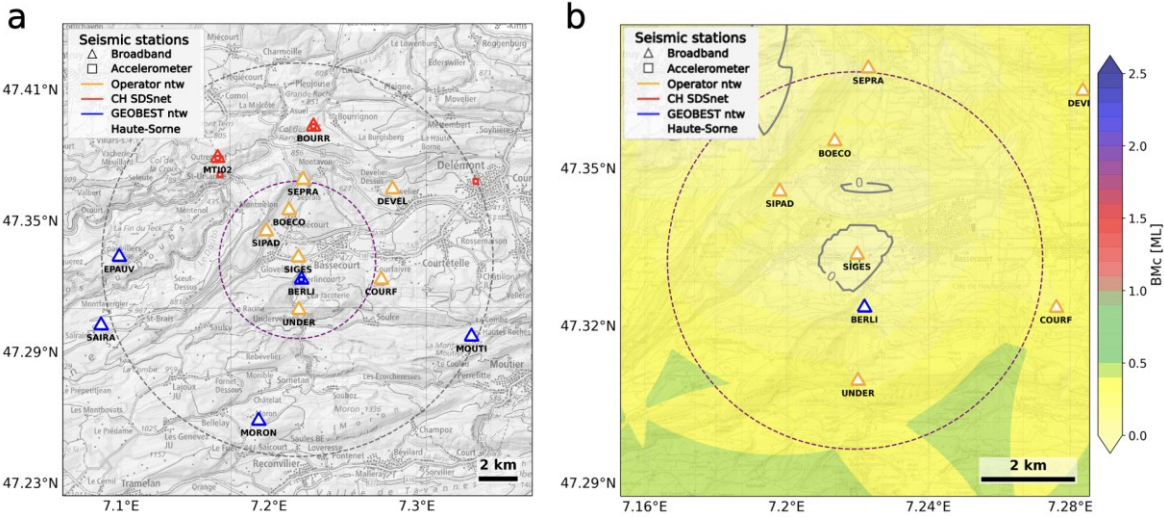


Figure 2: Network status and completeness as of July 2025. a) Stations of the monitoring network for the Haute-Sorne EGS project (Swiss Seismological Service, 1983; 2006; 2021). The dashed circles represent the 4 km alarming and 10 km deployment perimeters. b) Map of expected completeness for earthquakes, requiring at least four detecting stations, using the BMC method calibrated for Switzerland. The dashed circle represents the 4 km alarming perimeter in place during the July 2025 test stimulation. Isolines of  $M_L0.0$  completeness are marked in grey.

With the additional stations of the operator, the completeness of the full network approaches  $M_L0.0$  in the central perimeter as seen with the BMC modeling on Figure 2-b. This modeled completeness was tested during the test stimulation in July 2025, with events as low as  $M_{Lhc}0.1$  detected automatically by the SED processing system.

Figure 3 shows that an event with  $M_{Lhc}0.0$  at 5 km depth can still be located with a  $1\sigma$  accuracy lower than 500 m horizontally in large parts of the alarming perimeter, in particular around the wellhead. Overall, such an event can be located in all parts of the perimeter, with a  $1\sigma$  precision of 1000 m, both horizontally and vertically.

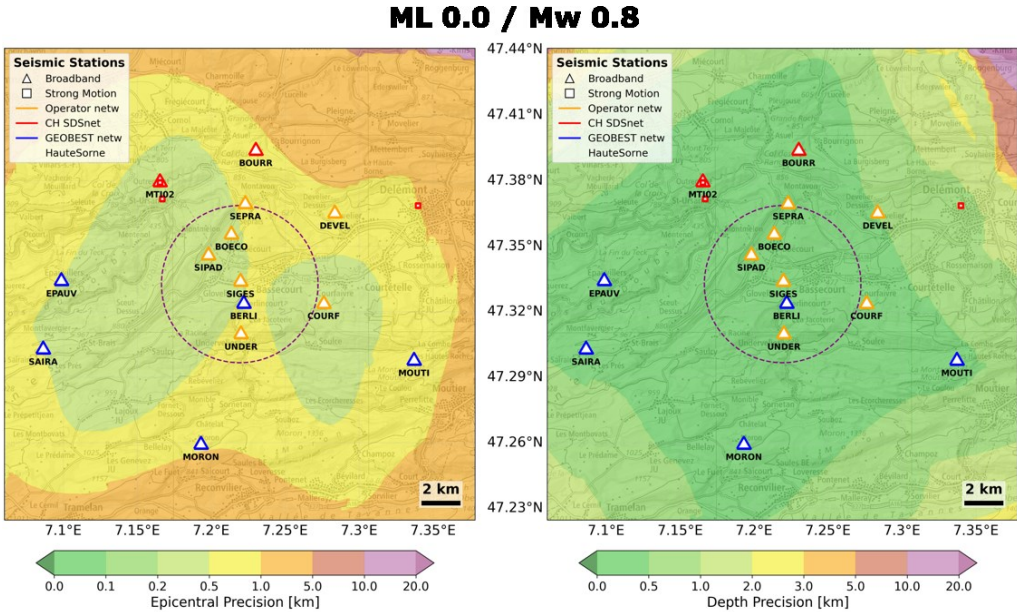


Figure 3: Maps of estimated location precision: Epicenter (left) and depth (right) for synthetic earthquakes of magnitudes  $M_L0.0$ . The color scale gives the location precision (in kilometers) at a  $1\sigma$  (68%) confidence level. Note that different color scales are applied to better reflect the SED guidelines recommendations for horizontal and vertical estimates.

### 3.3 Alarming system for the Haute-Sorne project

Table 1 gives an overview of the magnitude-based alarms thresholds of the traffic light system (TLS) in place for the test stimulation in July 2025. The conversion between  $M_{Lhc}$  (authoritative magnitude in Switzerland provided by the Swiss Seismological Service) and  $M_w$  (used by the operator) follows Edwards et al., 2025. The full TLS operated by Geo-Energie Jura and Geo-Energie Suisse in place during the test stimulation included geometrical and statistical parameters on top of the magnitude-based thresholds.

During the test stimulation in July 2025, the SED operated its alarming system in critical phase: For all events above the yellow TLS threshold, automatic alerts were sent by text message and email to project stakeholder (operators, SED, cantonal authorities) within 2-5 minutes of detection and manually revised alarms within 60 minutes. The alarming perimeter for automatic and manual detections consisted of a circle of radius 4 km centered at the wellhead. Both automatic and manual alerts were set up with a depth limit of 10 km in order to avoid triggering operational changes due to deep events known to occur in the area.

An additional alert for distant felt events was also in place for events with a magnitude at or above  $M_{Lhc}4$  in a radius of 20-25 km. Such events, even if unlikely to be linked to operations, could cause perturbations in the operations, slight damage to infrastructures, and raise concern in the population. This alarming perimeter was designed to include the area around the natural Réclère sequence, which saw two events of magnitudes  $M_{Lhc}4.1$  and  $M_{Lhc}4.3$  in December 2021 and March 2023 respectively (Diehl et al., 2024).

**Table 1: Overview of the magnitude-based traffic light system in place during the test stimulation in July 2025 for the EGS project in Haute-Sorne.**

	Green	Yellow	Orange	Red
Magnitude threshold ( $M_{Lhc}$ )	$M_{Lhc} < 0.25$	$0.25 \leq M_{Lhc} < 0.85$	$0.85 \leq M_{Lhc} < 1.5$	$M_{Lhc} \geq 1.5$
Magnitude threshold ( $M_w$ )	$M_w < 1.0$	$1.0 \leq M_w < 1.4$	$1.4 \leq M_w < 1.8$	$M_w \geq 1.8$
Action	Continue with program as designed	Temporary stop of injection for 6 hours	Stop injection, flowback if more than 3 additional orange events	Stop injection, flowback

## 4. SEISMIC CATALOGS

### 4.1 SED catalogue

Waveform data from all stations shown in Figure 2-a and additional stations of the Swiss national network (Swiss Seismological Service, 1983) are processed in real time using SeisComP (Helmholtz-Centre Potsdam - GFZ German Research Centre for Geosciences and gempA GmbH, 2008). Automatic event detection, location and magnitude is usually completed within 30s of an earthquake's occurrence, using at least six stations and only P-phase picks (Diehl et al., 2025). The SeisComP software is also used for manual review and repicking of all events. For the July 2025 stimulation test, the SED was operating in 'critical phase' mode, during which every event detected from the yellow TLS threshold was manually reviewed within 60 minutes of the alert (Table 1 and section 3.3).

Since 2020, the SED uses  $M_{Lhc}$  as its standard scale for (local) magnitude to account for the high density of the national network (Diehl et al., 2025). This revised local magnitude  $M_{Lhc}$  calibrated for Switzerland enables to accurately estimate magnitudes for smaller earthquakes as it is calibrated for seismic stations very close to the earthquake and takes into account physics-based site corrections. Locations are performed using the NonLinLoc algorithm and a national 3D velocity model (Lomax et al. 2000; Diehl et al., 2021).

For the four small events recorded during the July 2025 test stimulation, manual locations from the SED fixed the hypocenter to the coordinates of the borehole at a depth of 3.2 km below sea level in order to avoid bias in the magnitude estimation that would result from the location uncertainty for such small events, as the magnitude is relevant to the TLS operation. Later post-processing of the four events detected by the SED's routine system using at least 23 phases and 14 stations provided a depth range between 3.6 and 4 km, epicentral uncertainties lower than 275 m, and vertical uncertainties lower than 260 m. These calculated uncertainties on events ranging from  $M_{Lhc}0.1$  to  $M_{Lhc}0.3$  confirm the predicted results seen in Figure 3 for a  $M_{Lhc}0.0$  event and satisfies the requirements of the good-practice guide of a completeness of at least  $M_{Lhc}0.5$  (Kraft et al., 2025). Events detected and located by the SED routine system are automatically published in near-real-time in the SED catalogue and on the public webpage dedicated to the project, ensuring transparent communication to stakeholders and the public (<https://www.seismo.ethz.ch/en/monitoring/special-networks/geothermal-energy-haute-sorne/Recent-List-of-Earthquakes/>).

### 4.2 Template-matched catalog

Starting from the manually picked events in the SED catalogue, a quasi-real-time scan was set in place during and after the test stimulation using the QuakeMatch toolbox (Toledo et al., 2025). Single station template matching allows for the detection of previously missed small magnitude events by leveraging waveform similarity. The QuakeMatch workflow enables the dynamic addition of template as operations progress and performs both backward and forward scans. For the test stimulation in Haute-Sorne, the scan was set up on station 5A.SEPRA, which provided the best noise conditions despite not being the closest station from the wellhead (Figure 2-a), using three of the four manually located events as template (two events being too similar to provide any benefit; template events are marked by black rings in the bottom panel of Figure 4). Cross-correlation threshold was set at 0.5, meaning only detection highly similar to the template event were processed.

Figure 4 shows the timeline of events recorded by the surface network (grey histogram and circled in grey) and detection from the template-matching analysis. On the bottom panel, the ' $M_L$ ' magnitudes for detections are derived from fixed-slope regressions on template-family-

based  $M_L$ -vs-amplitude observations at the scanning station. One can estimate the achieved completeness of the SED routine locations by comparing them to the more complete template matched catalog, which shows the smallest detection captured by the SED routine system with a magnitude  $M_{Lhc}-0.1$ . Although the number of SED detected events is too low to properly assess the frequency magnitude distribution and completeness, this suggests that the completeness of the automatic SED catalog lies between  $\sim M_{Lhc}0.0$  and  $M_{Lhc}0.2$ , in line with the BMC predicted completeness of  $\sim M_{Lhc}0.0-0.3$  (Figure 2-b). Of the 70 events identified by template matching ranging from  $M_L-1.8$  to  $M_L0.3$ , 26 were subsequently located manually in SeisComp.

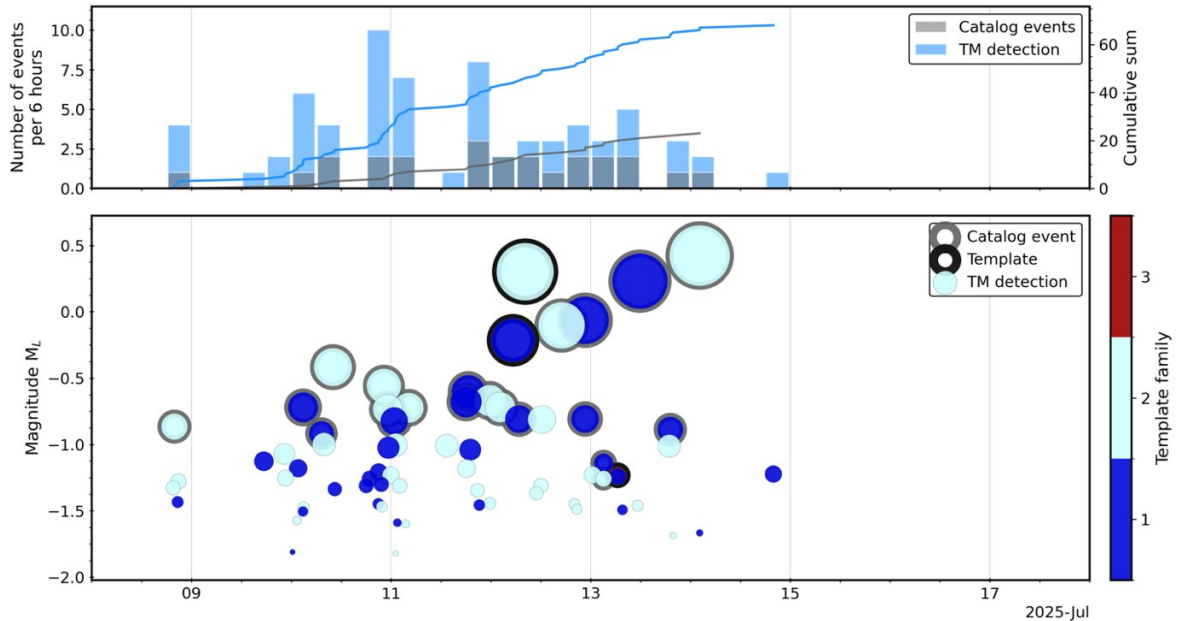


**Figure 4:** Near-real-time template matching for the Haute-Sorne test stimulation of July 2025. Top panel: Catalog events (grey) and template-matching detections (blue) per 6-hour bin, with cumulative counts on the right axis. Bottom panel: Magnitude-time distribution. Grey circles show catalog events, black circles templates, and filled circles template-matching detections that could not be located. Disk colors indicate the template family.

### 4.3 Categorization of seismic events

Both natural and induced seismicity have been detected in the vicinity of the EGS project in 2025, leading to the need for project stakeholders to decide on a categorization scheme. The SED took on this task and opted to use the E-PIE tool developed by Foulger et al., (2023) to support its assessment. The classification depends on temporal and spatial seismological and operational criteria, as well as additional information (focal mechanisms, precursory surface events, foreshock-aftershock patterns...). Figure 5 shows the E-PIE results for two events detected in 2025 around the geothermal project. The event in Figure 5-a is one of the four events detected during the test stimulation in July 2025, its E-PIE shows over 85% likelihood of the event being induced and this result was used by the SED to label the event as such in its database. The event in Figure 5-b occurred 3 months after the test stimulation, with an epicentral distance of only 400 m but at a depth of 17 km, much deeper than the operations. Its E-PIE suggests a natural origin with close to 60%; the relatively large share of ‘human induction’ in red is mainly driven by the event’s close epicentral proximity to the industrial project.

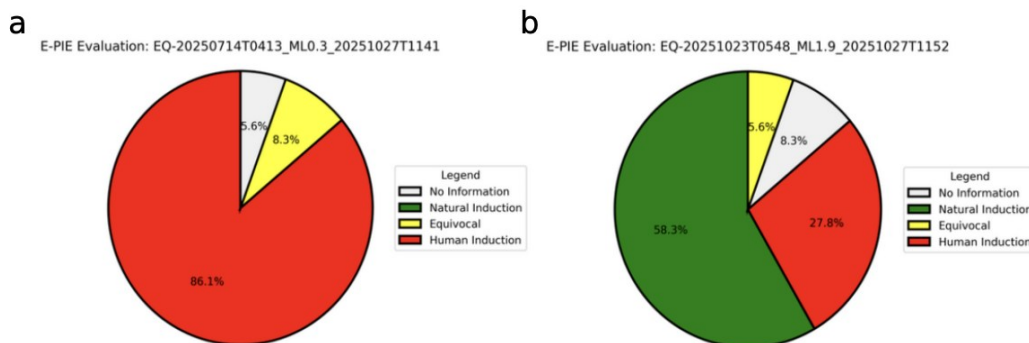


**Figure 5:** Examples of the use of the categorization scheme developed by Foulger et al. (2023) for two earthquakes that occurred in 2025 near the Haute-Sorne site. a) One of the two strongest earthquakes recorded during the stimulation test of July 14<sup>th</sup>, with a magnitude of  $M_{Lhc}0.3$ . b)  $M_{Lhc}1.9$  in the immediate vicinity of the site at a depth of 17 km, recorded on October 23<sup>rd</sup> (when no operations were taking place).

## 5. CONCLUSION

During the test stimulation of the pilot EGS project in Haute-Sorne, the Swiss Seismological Service provided an independent monitoring of the seismicity to all project stakeholders and the public. The deployment and continuous operation of a custom designed seismic network enabled the automatic detection, location and quantification of very small magnitude events, critical for the operation of the traffic light system by the industrial operator. Additional detection workflow using template-matching increased the number of events in the SED catalog significantly using existing stations, allowing for the verification of previously computed theoretical estimates of the magnitude of completeness and location accuracy of the seismic network. Finally, the application of a categorization scheme to determine the nature of seismic events advanced the near-real-time support that the SED can provide to cantonal authorities and project stakeholders.

By fostering cooperation between cantonal authorities and the SED, the GEOBEST program enables a climate of trust and transparency around the management of induced seismicity associated with deep geothermal projects. It serves as a springboard for project development by providing a framework of independent expertise, structured regulatory oversight, and real-time risk communication.

## REFERENCES

- Antunes, V., Kraft, T., Toledo, T., Reyes, C., Megies, T., & Wiemer, S. (2025). Optimising Seismic Networks for Enhanced Monitoring of Deep Geothermal Projects in Switzerland. *Proceedings European Geothermal Congress 2025*. <https://doi.org/10.3929/ethz-c-000791611>
- Bay, F., Wiemer, S., Fäh, D., & Giardini, D. (2005). Predictive ground motion scaling in Switzerland: best estimates and uncertainties. *Journal of seismology*. <https://doi.org/10.1007/s10950-005-5129-0>
- Bergamo, P., Sunny, J., Grigoratos, I., Roth, P., Kraft, T., Panzera, F., and Wiemer, S. (2005). Modelling soil response at the national scale for Switzerland in the framework of risk assessment of induced seismicity, EGU General Assembly 2025, Vienna, Austria, 27 Apr–2 May 2025, EGU25-8121, <https://doi.org/10.5194/egusphere-egu25-8121>, 2025.
- Bethmann, F., Alcolea, A., Dyer, B., Karvounis, D., Meier, P., Ollinger, D., & Zingg, O. (2025). Seismic Risk Mitigation for the Haute-Sorne EGS Pilot Project. *Proceedings European Geothermal Congress 2025*.
- Bommer, J. J., Oates, S., Cepeda, J. M., Lindholm, C., Bird, J., Torres, R., Marroquín, G., & Rivas, J. (2006). Control of hazard due to seismicity induced by a hot fractured rock geothermal project. *Engineering Geology*. <https://doi.org/10.1016/j.enggeo.2005.11.002>
- Diehl, T., Kissling, E., Herwegh, M., & Schmid, S. M. (2021). Improving Absolute Hypocenter Accuracy With 3D Pg and Sg Body-Wave Inversion Procedures and Application to Earthquakes in the Central Alps Region. *Journal of Geophysical Research: Solid Earth*. <https://doi.org/10.1029/2021JB022155>
- Diehl, T., Kraft, T., Mosar, J., Toledo, T., Lanza, F., & Simon, V. (2024). The ML4 Réclère Sequence (Switzerland): Evidence for Interaction of Reverse and Strike-Slip Faults in the Basement of the Jura Fold-and-Thrust Belt. *EGU 2024 - Copernicus Meetings*. <https://doi.org/10.5194/egusphere-egu25-16899>
- Diehl, T., Cauzzi, C., Clinton, J., Kraft, T., Kästli, P., Massin, F., Lanza, F., Simon, V., Grigoli, F., Hobiger, M., Roth, P., Haslinger, F., Fäh, D., & Wiemer, S. (2025). Earthquakes in Switzerland and surrounding regions during 2019 and 2020. *Swiss Journal of Geosciences*. <https://doi.org/10.1186/s00015-025-00489-4>
- Edwards, B., Kraft, T., Cauzzi, C., Philipp, K., & Wiemer, S. (2015). Seismic monitoring and analysis of deep geothermal projects in St Gallen and Basel, Switzerland. *Geophysical Journal International*. <https://doi.org/10.1093/gji/ggv059>
- Ellsworth, W. L. (2013). Injection-Induced Earthquakes. *Science*. <https://doi.org/10.1126/science.1225942>
- Foulger, G. R., Wilkinson, M. W., Wilson, M. P., Mhana, N., Tezel, T., & Gluyas, J. G. (2023). Human-induced earthquakes: E-PIE—a generic tool for Evaluating Proposals of Induced Earthquakes. *Journal of Seismology*. <https://doi.org/10.1007/s10950-022-10122-8>
- Grigoli, F., Cesca, S., Rinaldi, A. P., Manconi, A., Clinton, J. F., Westaway, R., Cauzzi, C., Dahm, T., & Wiemer, S. (2018). The November 2017 M w 5.5 Pohang earthquake: A possible case of induced seismicity in South Korea. *Science*. <https://doi.org/10.1126/science.aat2010>
- Grigoratos, I., Bergamo, P., Cauzzi, C. V., Danciu, L., Imtiaz, A., Roth, P., Sunny, J., & Wiemer, S. (2025). Extending ERM-CH23 to shallow induced seismicity in Switzerland. *ETH Zurich*. <https://doi.org/10.3929/ethz-b-000727014>
- Häring, M. O., Schanz, U., Ladner, F., & Dyer, B. C. (2008). Characterisation of the Basel 1 enhanced geothermal system. *Geothermics*. <https://doi.org/10.1016/j.geothermics.2008.06.002>
- Helmholtz-Centre Potsdam - GFZ German Research Centre for Geosciences and gempa GmbH (2008). The SeisComP seismological software package. *GFZ Data Services*. <https://doi.org/10.5880/GFZ.2.4.2020.003>
- Kraft, T., Mignan, A., and Giardini, D. (2013). Optimization of a large-scale microseismic monitoring network in northern Switzerland. *Geophysical Journal International*. <https://doi.org/10.1093/gji/ggt225>
- Kraft, T., Roth, P., Ritz, V. A., Antunes, V., Toledo, T., & Wiemer, S. (2025). Good-Practice Guide for Managing Induced Seismicity in Deep Geothermal Energy Projects in Switzerland. *ETH Zurich*. <https://doi.org/https://doi.org/10.3929/ethz-b-000714220>

- Lomax, A., Virieux, J., Volant, P., & Berge-Thierry, C. (2000). Probabilistic earthquake location in 3D and layered models: Introduction of a Metropolis-Gibbs method and comparison with linear locations. In *Advances in seismic event location*.
- Lupi, N., Ortet, S., & Ritz, V. A. (2025). Induced seismicity: a collaborative approach to safe geothermal energy development in Switzerland. *Proceedings European Geothermal Congress 2025*. <https://doi.org/https://doi.org/10.3929/ethz-c-000794687>
- Meier, P. M., Rodríguez, A., & Bethmann, F. (2015). Lessons Learned from Basel: New EGS Projects in Switzerland Using Multistage Stimulation and a Probabilistic Traffic Light System for the Reduction of Seismic Risk. *Proceedings World Geothermal Congress*.
- Meier, P., Zingg, O., El-Alfy, A., Bethmann, F., Castilla, R., Lübbers, B., Christe, F., Epiney, C., Heilig, J., Alcolea, A., Dyer, B., Karvounis, D., Ollinger, D., Fiori, R., Allenbach, R., Saati, W., Etter, M.-A., & Allimann, Y. (2025). First results from the exploration phase of the Haute-Sorne EGS project in Canton Jura, Switzerland. *Proceedings European Geothermal Congress 2025*.
- Merkofer, R., Brehme, M., & Shor, R. J. (2024). Evaluation of the geothermal energy potential of Switzerland - a techno-economic approach. *Proceedings 49th Workshop on Geothermal Reservoir Engineering*.
- Mignan, A., Werner, M. J., Wiemer, S., Chen, C. C., and Wu, Y. M. (2011). Bayesian Estimation of the Spatially Varying Completeness Magnitude of Earthquake Catalogs. *Bulletin of the Seismological Society of America*. <https://doi.org/10.1785/0120100223>
- Papadopoulos, A. N., Roth, P., Danciu, L., Bergamo, P., Panzera, F., Fäh, D., Cauzzi, C., Duvernay, B., Khodaverdian, A., Lestuzzi, P., Odabaşı, Ö., Fagà, E., Bazzurro, P., Marti, M., Valenzuela, N., Dallo, I., Schmid, N., Kästli, P., Haslinger, F., and Wiemer, S. (2024). The Earthquake Risk Model of Switzerland, ERM-CH23, *Nat. Hazards Earth Syst. Sci.*, 24, 3561–3578, <https://doi.org/10.5194/nhess-24-3561-2024>
- Swiss Seismological Service. (1983). National Seismic Networks of Switzerland [CH]. *ETH Zurich*. <https://doi.org/10.12686/SED/NETWORKS/CH>
- Swiss Seismological Service. (2006). GEOBEST Baseline Seismic Monitoring Networks for Deep Geothermal Energy Projects in Switzerland (G2). *ETH Zurich*. <https://doi.org/10.12686/SED/NETWORKS/G2>
- Swiss Seismological Service. (2021). Temporary Deployments operated by industry partners of the Swiss Seismological Service, typically associated with geothermal monitoring projects [5A]. *International Federation of Digital Seismograph Networks*. <https://doi.org/10.12686/sed/networks/5A>
- Toledo, T., Simon, V., Kraft, T., Diehl, T., & Antunes, V. (2025). Using waveform similarity to enhance the long-term analysis of a Swiss geothermal project. *Proceedings European Geothermal Congress 2025*. <https://doi.org/10.3929/ethz-c-000793890>
- Trutnevyte, E., & Wiemer, S. (2017). Tailor-made risk governance for induced seismicity of geothermal energy projects: An application to Switzerland. *Geothermics*. <https://doi.org/10.1016/j.geothermics.2016.10.006>
- van Elk J. Bourne S. J. Oates S. J. Bommer J. J. Pinho R., and Crowley H. 2019. A probabilistic model to evaluate options for mitigating induced seismic risk, *Earthq. Spectra*. <https://doi.org/10.1193/050918EQS118M>

## ACKNOWLEDGEMENTS

Authors from the second on are listed in alphabetical order. The work of SED for the Haute-Sorne EGS pilot project is supported by the GEOBEST2020+ program, funded by the Swiss Federal office of Energy. The authors are grateful for the support of the SED's elab, network, communication, and IT groups.